Unusual properties of ruthenium(II) diphenylcyanamide complexes: chemistry and application as sensitizers of nanocrystalline TiO_2

Stefan Ruile,* Oliver Kohle, Henrik Pettersson and Michael Grätzel

Institut de Chimie Physique, Ecole Polytechnique Fédérale de Lausanne, CH-1015 Lausanne, Switzerland

In this study, a series of ruthenium(II) polypyridyl complexes of the general formula $Na_4[Ru^{II}(dcbpy)_2X_2]$ (dcbpy is 2,2′-bipyridine-4,4′-dicarboxylate and X is a substituted phenylcyanamide anion) are investigated. When introduced into the ruthenium co-ordination sphere, the phenylcyanamide ligand showed linkage isomerism and was co-ordinated *via* the nitrile- or amide nitrogen, as shown by ^{1}H NMR, ^{13}C NMR spectroscopy and use of a ^{13}C-labeled ligand. The title compounds exhibited unusually high first pK_a values between 5 and 6, determined *via* spectrophotometric titrations. The first protonation occurred at the phenylcyanamide ligand, rendering the energy of the lowest energy ^{1}MLCT absorption strongly pH-dependent. In photovoltaic devices, overall efficiencies were in the range of 3–4%, due to photon-to-current conversion efficiencies of 50–60% at 520 nm. The long-term stability of a representative complex under irradiation was investigated in solution and in a solar cell device.

The potential of dye-sensitized titanium dioxide electrodes in solar-to-electrical energy conversion schemes is considerable. Demonstrated solar energy conversion efficiencies of 10% are promising under the aspect of an industrial application of the photoelectrochemical cell.[1,2]

Ruthenium(II) 2,2′-bipyridine-4,4′-dicarboxylic acid ($dcbpyH_2$) complexes are the most frequently used sensitizers for TiO_2, due to their favorable light absorption, electrochemical and photoelectrochemical properties, and their photostability in the device.[3–8] In particular, *cis*-$Ru(dcbpyH_2)_2(NCS)_2$, **1**, showed an unmatched conversion efficiency in solar cell devices.[2] The main reasons for this lie in an apparently perfectly positioned π* energy level, a relatively high-lying Ru (t_{2g}) energy level, a favorable geometry and size of the molecule, and in the presence of the two thiocyanate ligands. Most of the efficient ruthenium polypyridine sensitizers contain this ligand, as it seems to support quantitative electron injection.[7] Four carboxylic acid groups enhance the absorption coefficients of the MLCT transitions. The limitation of ruthenium polypyridyl sensitizers is, however, their small absorption coefficients at longer wavelengths (above 700 nm).

In complexes of the type $Ru(dcbpy)_2X_2$, absorption properties are mainly controlled by the donor strength of the ligand X. A strong electron donor destabilizes the ruthenium ground state energy level (t_{2g} level), giving rise to MLCT transitions shifted to lower energies.[9,10] Hence a promising approach to a more efficient sensitizer is to replace the thiocyanate ligands in **1** by stronger electron donors. Substituted phenylcyanamide anions are candidates for this purpose.[8] Their donor strength may in addition be fine-tuned by a judicious choice of the substituents at the phenyl ring.[11]

The long-term stability of the dye is a key requirement when an industrial application as a sensitizer for TiO_2 in a solar cell device is considered. For a long time, it was questioned whether ruthenium polypyridine complexes could fulfill the strenuous requirement of millions of turnovers without decomposition. Such a long-term stability in a solar cell device could only recently be shown for **1**.[12,13] However, under irradiation in solution, **1** decomposed with loss of sulfur.[13,14]

In the present study, the synthesis, chemistry and photoelectrochemistry of a series of ruthenium polypyridyl complexes containing two phenylcyanamide ligands are reported. The stability of the new complexes under irradiation is studied in solution and in a photovoltaic cell.

Experimental

Materials

All solvents and chemicals used were at least reagent grade and were purchased from Fluka AG or Aldrich (Switzerland). Sephadex LH-20 was obtained from Pharmacia. Electrodes were coated with nanocrystalline TiO_2 prepared *via* a sol-gel procedure.[15] The molten salts HM_2I (3-hexyl-1,2-dimethylimidazolium iodide) and HMI (1-hexyl-3-methylimidazolium iodide) were synthesized in a similar manner as previously reported.[16] The phenylcyanamide ligands were prepared from substituted anilines *via* the thiourea route.[17] A sample of ^{13}C-labeled thallium 4-chlorophenylcyanamide was available from a previous study.[8] *cis*-$Ru(dcbpyH_2)_2Cl_2$, **2**, was a gift of Solaronix SA (Aubonne, Switzerland). Elemental analyses were carried out by the analytical service of Ciba-Geigy (Basel, Switzerland).

$Na_4[Ru(dcbpy)_2(2\text{-}Clpcyd)_2]$, 3. **2** (90 mg) was dissolved in a mixture of 0.5 M aqueous NaOH (20 mL) and dimethylformamide (45 mL). Subsequently 2-chlorophenylcyanamide (435 mg) was added and the reaction mixture was refluxed for 4 h. After cooling to room temperature, the solvent was evaporated and the product was purified on a short Sephadex LH-20 column. The product band was collected and evaporated to dryness. Then the solid was redissolved in methanol (10 mL), and diethyl ether was slowly added until the product precipitated. The solid was filtered off, washed with small amounts of a 5 : 2 diethyl ether–methanol mixture and dried *in vacuo*. Yield: 96 mg (62%). Anal. calcd. (%) for $C_{38}Cl_2H_{20}N_8Na_4O_8Ru \cdot 12H_2O$: C, 38.14; H, 3.71; N, 9.36. Found: C, 37.74; H, 3.32; N, 9.16.

$Na_4[Ru(dcbpy)_2(4\text{-}Clpcyd)_2]$, 4. **4** was prepared in the same way as **3**, starting from 200 mg of **2** and 900 mg of 4-chlorophenylcyanamide. Yield: 171 mg (54%). Anal. calcd. (%) for $C_{38}Cl_2H_{20}N_8Na_4O_8Ru \cdot 6.5H_2O$: C, 41.58; H, 3.03; N, 10.21. Found: C, 41.55; H, 3.32; N, 10.26.

$Na_4[Ru(dcbpy)_2(2,4,5\text{-}Cl_3pcyd)_2]$, 5. The preparation from 80 mg of **2** and 470 mg of 2,4,5-trichlorophenylcyanamide was identical to the one of **3**. Yield: 80 mg (56%). Anal. calcd. (%) for $C_{38}Cl_6H_{16}N_8Na_4O_8Ru \cdot 7H_2O$: C, 36.68; H, 2.43; N, 9.00. Found: C, 36.95; H, 2.85; N, 8.91.

$Na_4[Ru(dcbpy)_2(2,4,6\text{-}Cl_3pcyd)_2]$, 6. **6** was prepared like **3**, with 80 mg of **2** and 500 mg of 2,4,6-trichlorophenylcyanamide as starting materials. Yield: 64 mg (49%). Anal. calcd (%) for $C_{38}Cl_6H_{16}N_8Na_4O_8Ru \cdot H_2O$: C, 40.16; H, 1.60; N, 9.86. Found: C, 40.17; H, 1.55; N, 9.52.

$Na_4[Ru(dcbpy)_2(3,5\text{-}Cl_2pcyd)_2]$, 7. The synthesis was identical to the one of **3**, starting from 82 mg of **2** and 480 mg of 3,5-dichlorophenylcyanamide. Yield: 78 mg (55%). Anal. calcd (%) for $C_{38}Cl_4H_{18}N_8Na_4O_8Ru \cdot 8H_2O$: C, 38.24; H, 2.87; N, 9.39. Found: C, 38.15; H, 2.47; N, 9.27.

Methods

Spectroscopic studies. ^1H and ^{13}C NMR spectra were measured on a Bruker AC-P 200 spectrometer. Chemical shifts are given in ppm, relative to tetramethylsilane. The pulse repetition time in ^{13}C NMR measurements was 3 s. UV/VIS spectra were obtained on a Hewlett Packard 8452A diode array spectrophotometer. Emission spectra were measured on Perkin-Elmer LS 50 B luminescence spectrometer. Fourier transform infrared spectra were recorded from KBr pellets on a Perkin-Elmer Paragon 1000 FTIR spectrophotometer. Spectrophotometric titrations were performed in 10^{-5} M aqueous dye solutions. Their ionic strength was kept constant at a value of one with a phosphate–citrate buffer. After adjusting the pH value with dilute HCl, solutions were stirred for at least one minute until the equilibrium was attained.

Electrochemistry. Cyclic voltammetry was performed in argon-purged DMSO, dried over a molecular sieve, in the presence of 0.1 M tetrabutylammonium trifluoromethanesulfonate as the supporting electrolyte. In the three-electrode setup, a glassy carbon working electrode (surface 0.07 cm^2), a glassy carbon counter electrode (separated from the working electrode compartment by a bridge containing the same electrolyte as the test solution), and a silver wire as a quasi-reference electrode were used. The quasi-reference electrode was calibrated with a Ag/AgCl/KCl saturated reference electrode. Reported potentials refer to the latter. Scan rates between 100 and 300 mV s^{-1} were used.

Photoelectrochemical measurements. TiO_2 electrodes were coated for 15 h under exclusion of light in 5×10^{-4} M ethanolic dye solutions at room temperature. If there was no deep coloration of the electrode, soaking was continued for 2 h at 70 °C. Unless otherwise stated, the dye solutions contained 50 mM of 3α,7β-dihydroxy-5β-cholanic acid as a coadsorbate. As the electrolyte, a mixture containing 0.6 M HM_2I, 40 mM of I_2, 40 mM of LiI and 200 mM of 4-*tert*-butylpyridine in acetonitrile was used. The setup and procedure for the measurement of action spectra and current–voltage characteristics are described elsewhere.[2]

Stability. The long term performance of **3** was studied with semi-transparent cells of a surface area of 1 cm^2, sealed with an epoxy resin. The cells were prepared following the general procedure for the fabrication of dye-sensitized, nanocrystalline solar cells.[2,18] Three sets of cells were prepared. In the first, the working electrodes were sensitized with a 3×10^{-4} M ethanolic solution of **3**. The second set was coated in the same way, except that the solutions contained in addition 50 mM 3α,7β-dihydroxy-5β-cholanic acid. For the third set, sensitizer **1** was used as a dye. Each set consisted of five cells. HMI containing 300 mM of 4-*tert*-butylpyridine and 10 mM of I_2 was used as an electrolyte. This experimental setup is useful to fabricate regenerative photoelectrochemical cells for low-power applications.[12]

During stability tests, cells were illuminated with a light source of 5000 lx (AM 1 is ≈120000 lx) under a polycarbonate UV filter. The cell temperature was kept constant at 50 °C. Current–voltage characteristics were measured using a 60 W incandescent lamp at a light intensity of 50 lx.

Results and discussion

Synthesis

Starting from the dichloro compound $Ru(dcbpyH_2)_2Cl_2$, **2**, two reaction pathways to the desired diphenylcyanamide complexes of the general formula $Na_4[Ru(dcbpy)_2(pcyd)_2]$ were tested: one involved the direct reaction of **2** with an excess of protonated phenylcyanamide ligand in a DMF–NaOH mixture; in the other, the thallium(I) salt of phenylcyanamide was used in 2.5 molar excess. Dimerization of phenylcyanamide was not a problem under the applied reaction conditions, as the ligand was found to be introduced in the complex exclusively in its monomeric, anionic form. Hence, the first route was preferred, as it avoids the very toxic thallium(I) compounds.

The phenylcyanamide complexes were subsequently passed over a short Sephadex LH-20 column and isolated as the tetrasodium salts by precipitation with diethyl ether from methanol. This procedure gave rise to products showing satisfactory elemental analyses.

The described procedure failed for more basic phenylcyanamide ligands, such as 4-(*N*-diethylamino)phenylcyanamide or 2,4,6-trimethylphenylcyanamide. In these cases, resulting complexes showed strongly blue-shifted absorption maxima at around 470 nm, suggesting incorporation of the ligands in the protonated form.

NMR spectra and bonding mode of phenylcyanamide

^1H NMR spectra of complexes **3** and **4** are presented in Fig. 1. All products were free of uncoordinated phenylcyanamide ligand, which would appear upfield shifted. Complete ^1H NMR data can be found in Table 1.

The 2,2-bipyridine-4,4-dicarboxylate signals show a pattern confirming the *cis* geometry of the complexes, where the pyridine units of each ligand are inequivalent, but each is equivalent to one pyridine ring of the other bipyridine.[19] These spectra thus contain signals of six distinguishable hydrogens. Their positions are only weakly affected by the nature of the phenylcyanamide ligand. The occurrence of only six bipyridine signals confirms the presence of one compound, in which

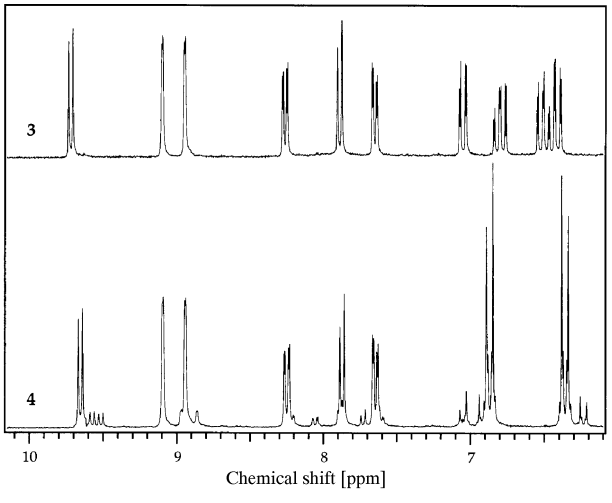

Fig. 1 Aromatic region of the ^1H NMR spectra of complexes **3** and **4**, measured in [$^2H_4$]methanol

Table 1 ^{1}H NMR data of complexes **3** – **7** in [$^2H_4$]methanol

	3	**4**	**5**	**6**	**7**
3	9.10 d (2) 1.2	9.10 s (2)	9.13 d (2) 1.1	9.04 d (2) 1.4	9.13 d (2) 1.1
5	8.26 dd (2) 5.8, 1.5	8.24 dd (2) 5.8, 1.4	8.30 dd (2) 5.7, 1.6	8.23 dd (2) 5.7, 1.6	8.28 dd (2) 5.8, 1.5
6	9.72 d (2) 5.8	9.66 d (2) 5.8	9.67 d (2) 5.9	9.73 d (2) 5.9	9.62 d (2) 5.7
3′	8.95 d (2) 1.3	8.95 s (2)	8.97 d (2) 1.3	8.89 d (2) 1.3	8.97 d (2) 1.3
5′	7.65 dd (2) 5.7, 1.6	7.65 dd (2) 5.9, 1.5	7.67 dd (2) 5.9, 1.6	7.60 dd (2) 5.8, 1.6	7.67 dd (2) 5.8, 1.6
6′	7.89 d (2) 5.8	7.88 d (2) 5.8	7.89 d (2) 5.8	7.77 d (2) 5.9	7.87 d (2) 5.8
pcyd	3*: 7.05 dd (2) 7.8, 1.5	3*, 5*: 6.87 m (4)	3*: 7.19 s (2)	3*, 5*: 7.00 s (4)	4*: 6.52 t (2) 1.7
pcyd	4*: 6.54 m (2)	2*, 6*: 6.36 m (4)	6*: 6.41 s (2)		2*, 6*: 6.25 d (4) 1.7
pycd	5*: 6.80 m (2)				
pcyd	6*: 6.41 dd (2) 8.0, 1.5				

the two bipyridine units have an identical chemical environment, which implies that the two phenylcyanamide ligands are co-ordinated in the same mode. This is the case for the complexes **3**, **5**, and **6**, which have in common a chloro substituent in the 2 position of the phenylcyanamide ligand. Due to the asymmetric C—N stretching vibrations in the infrared spectra at about 2170 cm^{-1}, it is concluded that both phenylcyanamide ligands are co-ordinated *via* the nitrile nitrogen.[20]

The proton NMR spectra of the 4-chlorophenylcyanamide complex **4** and of the 3,5-dichlorophenylcyanamide derivative **7** show a slightly different pattern in both spectra, additional signals occur. The position of the 2,2-bipyridine-4,4-dicarboxylate 6H proton signal, which is the most downfield shifted, gives further hints on the nature of the second compound. The NMR spectra show the occurrence of two new doublets of identical intensity. In complexes of the type $Na_4[Ru(dcbpy)_2XY]$, the two bipyridine units are in a different chemical environment, hence each of them shows its own set of signals. The presented NMR spectra of **4** and **7** thus indicate the presence of two differently co-ordinated phenylcyanamide ligands (signal integration reveals the incorporation of two bipyridine and two phenylcyanamide units), tentatively assigned to amide- and nitrile-bound, respectively. Structures of the two isomeric complexes are depicted in Fig. 2.

Linkage isomerism in this system is known for the dithiocyanate complex **1**, whose samples always contain a few percent of the isomer in which one thiocyanate ligand is *S*-bound.[7] In order to confirm linkage isomerism of the phenylcyanamide ligand, a sample of complex **4**, with ^{13}C-labeling at the cyanamide carbon, was prepared from **2** and ^{13}C-labeled thallium 4-chlorophenylcyanamide. The reaction time was, however, limited to 90 min, as, at least in other complexes such as the previously studied Na[Ru(bmipy)(dcbpy)(4-Clpcyd)] [bmipy is 2,6-bis(1-methylbenzimidazol-2-yl)pyridine], prolonged refluxing favored the formation of nitrile-co-ordinated phenylcyanamide.[8] The proton NMR spectrum of the ^{13}C-labeled compound revealed an isomer content of around 10%. The ^{13}C NMR spectra of the labeled and the unlabeled complex are compared in Fig. 3. They show some marked differences due to the ^{13}C-labeling. The weak signals appearing at 129.6 ppm are assigned to phenyl signals of the phenylcyanamide ligand, as they appear in the spectral region between 126 and 135 ppm.[21] Low intensity signals at around 123.5 ppm might be due to 5 and 5′ carbon atoms on the bipyridine ligand.[22] In unlabeled samples, the cyanamide carbon signal is not visible due to its lower spectral sensitivity, compared with the phenyl carbon atoms. The isotope-labeled compound shows, apart from the phenyl carbon signals, three additional peaks. The main signal at 130.0 ppm is due to *N*-bound phenylcyanamide in the double nitrile-bound isomer, and two smaller peaks at 130.6 ppm and 125.4 ppm show the nitrile- and amide-co-ordinated ligands in the mixed isomer, respectively. The signal at 130.6 ppm is typical for carbodiimides and the one at 125.4 ppm appears in a spectral region usually assigned to organonitriles.[8,23]

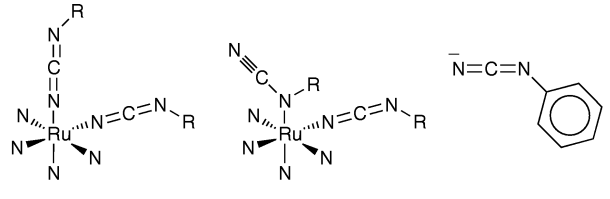

Fig. 2 Structures of the diphenylcyanamide complexes $[Ru(dcbpy)_2(pcyd)_2]^{4-}$. Only the nitrogen atoms of the dcbpy ligands are shown. Left: major isomer. Middle: mixed isomer. Right: free phenylcyanamide ligand (deprotonated form)

Absorption properties

Absorption spectra of the diphenylcyanamide complexes **3**–**7** are dominated by strong ligand-centered absorptions at 310 nm and two ^{1}MLCT maxima. The position of the lower energy ^{1}MLCT band maximum varies between 514 nm (**5**) and 530 nm (**6**) and yields absorption coefficients of around 12000 M^{-1} cm^{-1}. Emission maxima occur between 760 and 785 nm in methanol. Spectroscopic data can be found in Table 2.

The investigated complexes show only weak solvatochromism, but spectral changes on pH variation were dramatic. These effects were scrutinized in spectrophotometric titrations of the di-4-chlorophenylcyanamide complex **4** in water. In Fig. 4, absorption spectra at various pH values are displayed. Lowering the pH of the test solution was accompanied by an impressive color change from red-violet to bright orange. The fact that only the MLCT maxima were affected, but not the bipyridine-centered transitions, reveals that the variations must have their origin in a phenylcyanamide protonation. The spectral changes directly reflect the lower donor strength of

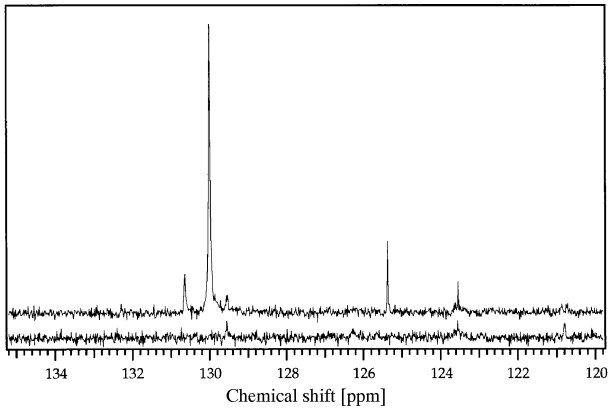

Fig. 3 ^{13}C NMR spectra of a ^{13}C-labeled sample (upper curve) and an unlabeled sample (lower curve) of complex **4** in [$^2H_4$]methanol

Table 2 UV/VIS, emission, IR, and electrochemical data

Complex	UV/VIS data[a] λ/nm (ε/10^3 M^{-1} cm^{-1})				Emission[a] λ/nm	Redox potentials[b] E_{ox}/mV	E_{red}/mV	IR[c] ν/cm^{-1}
3	524 (12.0)	384 (14.5)	310 (51.4)	302 (45.6)	785	450	−1540	2166
4	524 (11.6)	378 (15.0)	310 (54.9)	298 (52.1)	780	405	−1560	2180
5	516 (12.0)	376 (14.4)	310 (57.0)	298 (55.6)	775	560	−1525	2181
6	530 (11.8)	384 (14.5)	310 (58.7)	302 (54.0)	770	460	−1560	2174
7	514 (12.2)	376 (14.3)	310 (57.9)	300 (52.6)	775	540	−1510	2179

[a] In methanol. [b] *Versus* Ag/AgCl/NaCl satd, measured in DMSO; all waves were quasi-reversible. [c] KBr pellet.

protonated phenylcyanamide, compared with the deprotonated form.[24]

The origin of these changes is in the protonation/deprotonation equilibra given in equations (1) and (2):

$$[Ru(dcbpy)_2(4\text{-}Clpcyd)_2]^{4-} \underset{-H^+}{\overset{+H^+}{\rightleftharpoons}} [Ru(dcbpy)_2(4\text{-}Clpcyd)(4\text{-}ClpcydH)]^{3-} \quad (1)$$

$$[Ru(dcbpy)_2(4\text{-}Clpcyd)(4\text{-}ClpcydH)]^{3-} \underset{-H^+}{\overset{+H^+}{\rightleftharpoons}} [Ru(dcbpy)_2(4\text{-}ClpcydH)_2]^{2-} \quad (2)$$

There are no examples of investigations of the acid-base properties of phenylcyanamide ruthenium(II) complexes in the literature. However, there are some studies on the cyanide ion. In the complex $M(bpy)_2(CN)_2$ (M = Ru, Fe) the cyanide ligand showed appreciable proton affinity (yet pK_a values were below one), and both the mono- and the di-protonated species could be identified.[25] Their presence was verified by the occurrence of two sets of isosbestic points. No clear isosbestic points would have indicated that the mixture contained more than two compounds at the same time.

The same analytical method was applied for the phenylcyanamide complex **4**. In Fig. 5, spectra at pH values between 8.10 and 6.22 are shown. Lowering of the pH in that range yielded a blue-shifted absorption maximum of both ^{1}MLCT maxima, accompanied by a loss in absorption coefficient. A set of isosbestic points at 496, 440, 364, 324, 308 and 296 nm confirmed the presence of only two species, which are the deprotonated and the monoprotonated form, as given in equation (1). The subsequent lowering of the pH to 5.11 resulted in a

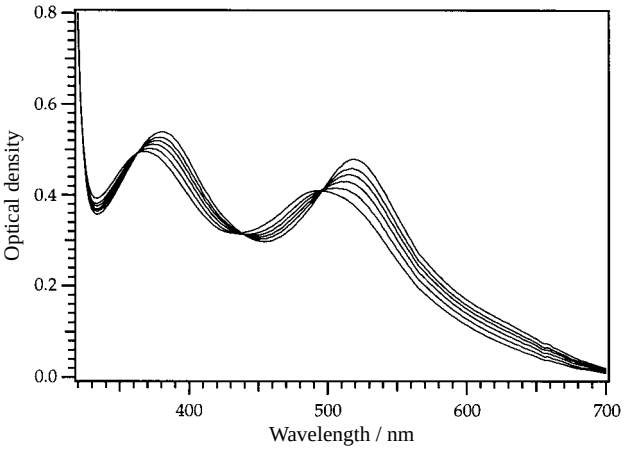

Fig. 5 ^{1}MLCT absorption bands of **4** at pH values of 8.10, 7.13, 6.86, 6.65, 6.45 and 6.22. The curve with the highest absorption was measured at pH 8.10

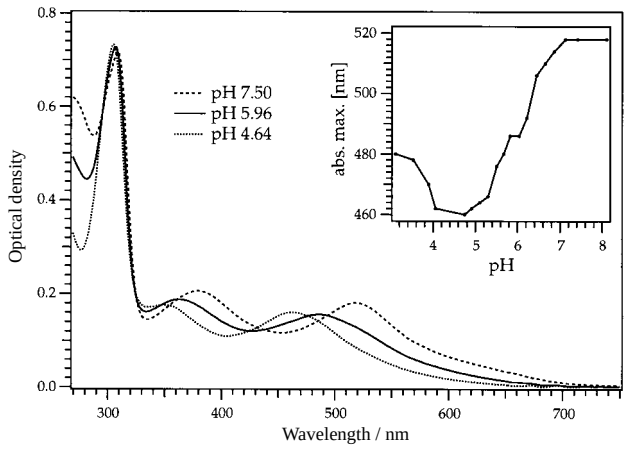

Fig. 4 Absorption spectra of complex **4** at various pH values in water. Insert: dependence of the ^{1}MLCT absorption maximum on solution pH

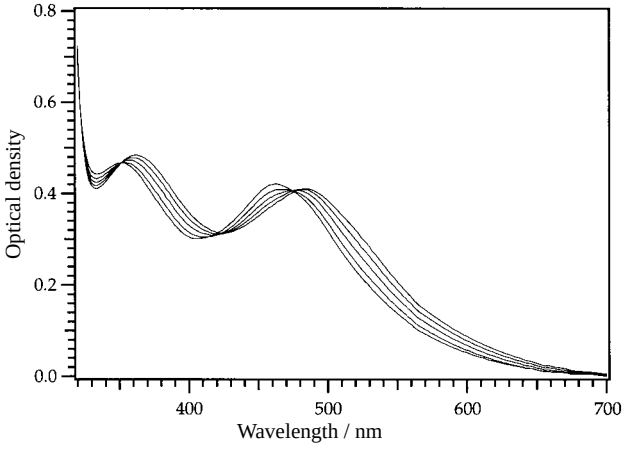

Fig. 6 ^{1}MLCT absorption bands of **4** at pH values of 5.83, 5.67, 5.51, 5.30 and 5.11. The curve with the lowest energy absorption maximum was measured at pH 5.83

further shift of the ^{1}MLCT maxima to higher energies. The spectra given in Fig. 6, measured at pH values between 5.11 and 5.83, contained a second series of isosbestic points at 476, 420, 352, 322, 308 and 293 nm. The protonation process is given in equation (2). Curves measured at pH values between 5.92 and 6.11 did not coincide with any isosbestic point, revealing that, at such pH values, species in all three protonation states are present in the solution. The insert in Fig. 4 shows the pH dependence of the ^{1}MLCT absorption maximum. Further lowering of the solution pH gives a red-shift of the lowest energy ^{1}MLCT maximum, due to protonation at the carboxylate group. The latter is also manifested by a shift of the bipyridine-centered π–π* absorption to 316 nm.

In order to estimate the pK_a value of **4**, relative absorption changes at the ^{1}MLCT maxima of the fully deprotonated compound (518 nm) and the di-protonated species (maximum at 460 nm) were calculated. A plot of the absorbance change *vs.* solution pH yielded complex pK_a values of 6.4 and 5.4.

The phenylcyanamide complexes can also be prepared in their protonated form by precipitation from aqueous solution by the addition of dilute HCl. Samples prepared in this way contained, as expected from the experiments described above, the phenylcyanamide ligands in their protonated form. Infrared spectra of **7**, precipitated as the tetrasodium salt, showed the typical very strong and broad band at 2179 cm^{-1} for the asymmetric C—N stretching vibration. However, after dissolving the same complex in water and precipitating it with dilute HCl, a completely different infrared spectrum was obtained. The C—N band was split into two new bands of low intensity at 2170 and 2262 cm^{-1}. Furthermore, a weak absorption at 3077 cm^{-1} occurred, which was assigned to an N—H stretching vibration.

As a consequence of the pH-dependent behavior, the phenylcyanamide complexes were exclusively used in their fully deprotonated form when operating in solar cell devices to ensure an optimal light harvesting at longer wavelengths. Furthermore, it should be noted that the phenylcyanamide ligand in its anionic form is expected to be more strongly bound to the ruthenium center.

Electrochemistry and photoelectrochemistry

Phenylcyanamide complexes **3**–**7** displayed very similar electrochemical behavior. At sweep rates between 100 and 500 mV s^{-1}, all oxidation and first reduction waves were quasi-reversible, with a peak separation between 100 and 130 mV. The oxidation potentials were measured to be between 405 and 560 mV *vs.* Ag/AgCl/NaCl satd (which has a potential of 192 mV *vs.* NHE). The first reduction occurred between −1510 and −1555 mV *vs.* Ag/AgCl/NaCl satd. Electrochemical data are listed in Table 2.

The complexes were tested as sensitizers for nanocrystalline TiO_2. Current–voltage characteristics and overall cell efficiencies were obtained with a thin-layer sandwich-type cell under illumination with simulated AM 1.5 solar light. The incident monochromatic photon-to-current conversion efficiency is derived from equation (3):[2]

$$\mathrm{IPCE}(\%) = \frac{(1.25 \times 10^3 \cdot \text{photocurrent density}(\mu\text{A cm}^{-2})}{\text{wavelength (nm)} \cdot \text{photon flux (W cm}^{-2})} \cdot 100 \quad (3)$$

Reported IPCE values (Table 3) are not corrected for light losses due to reflection or absorption by the supporting electrode. All presented values are the average of three measured electrodes. IPCE values at wavelengths above 550 nm depend strongly on the film thickness[2] of TiO_2, which was 9 μm in this work.

For all phenylcyanamide complexes, short-circuit currents did increase in a non-linear fashion with light intensity, indicating surface aggregation. Hence, 50 mM 3α,7β-dihydroxy-5β-cholanic acid was added to the ethanolic solutions of the dyes before soaking the electrodes. Cholanic acids have been shown to improve both the photocurrent and voltage of copper chlorophyllin-sensitized TiO_2 cells.[26] For the phenylcyanamide complexes, the same effect was observed. Device efficiencies reported in Table 3 were over three percent with all complexes except **7**. Complex **3** showed the highest open-circuit voltages and the best fill factors, hence yielding the highest cell efficiencies. Spectral characteristics of the investigated dyes are similar. Maximum injection efficiencies were at 47–61%, whereas at 700 nm, values of around 20% were measured. The redox potentials are obviously in a range to allow for efficient charge injection and dye regeneration, and hence are not responsible for reduced cell efficiencies. The results underline the importance of a quantitative light-to electrical energy conversion efficiency at shorter wavelengths between 400 and 600 nm in order to obtain high device efficiencies.[7]

The main reason for the reduced IPCE values of the diphenylcyanamide complexes, compared with the dithiocyanate complex **1**, is probably surface aggregation that was not completely suppressed, even by the presence of additives. The aggregated dye on the surface might cause a mass transport problem by blocking the semiconductor pores. This is supported by the observation that cell efficiencies are higher under low light intensities. Another reason may be that the complexes catalyze the dark current.

Stability

The stability of complex **4** in solution was studied under irradiation in quartz cells or NMR tubes with a 420 nm cut-off UV filter, while being kept at room temperature in a water bath. Combining absorption and NMR data reveals that in 0.25 M NaOH solution, a fast photocatalytic conversion of **4** to the complex $[Ru(dcbpy)_2(OH)_2]^{4-}$ occurs, while in methanolic solution, multiple products are formed, manifested by NMR spectra and a slight blue-shift of the ^{1}MLCT absorption maximum to 506 nm.

Table 3 Photoelectrochemical data under one sun illumination

Complex	IPCE(max) %	IPCE (700 nm) %	η/ %[a]	U_{oc} (mV)[b]	I_{sc} /mA cm^{-2} [c]	FF /mA cm^{-2} [d]
3	55	22	3.7	660	8.7	0.65
4	61	16	3.0	625	8.7	0.55
5	52	23	3.1	640	7.8	0.63
6	50	23	3.1	660	7.4	0.65
7	47	17	2.6	620	6.7	0.63

[a] Solar cell efficiency. [b] Open-circuit voltage. [c] Short-circuit current. [d] Fill factor.

The long term stability of **3** in the photovoltaic device under irradiation was studied with semi-transparent cells, sealed with an epoxy glue. Three sets of cells were investigated. The first one only contained **3** and the second one contained **3** with a cholanic acid derivative as co-adsorbate. As the photostability of cholanic acids is known to be limited, the two sets of cells containing **3** were prepared, in order to avoid a misinterpretation of decomposition effects of the additive. The third set was sensitized with **1** and was used as a reference. Resulting average open-circuit photovoltages and short-circuit currents are displayed in Fig. 7. Initial photovoltages directly reflect TiO_2 conduction band position engineering by protons present in the sensitizer solutions. The highest open-circuit voltage of 475 mV was reached with the proton-free **3**, whereas the use of the tetraprotonated **1** lowered the potential by about 30 mV. The addition of the cholanic acid derivative diminished the potential by 80 mV. However, the positive effect of the additive was visible in the short-circuit currents, which were nearly doubled in comparison with the cells containing **3** without additive. The highest currents of over 10 μA cm^{-2} were obtained with **1**. Fill factors were at around 0.70 mA cm^{-2} for all cells. The standard deviations of these values were extremely low, confirming the high reproducibility of the system. These current–voltage characteristics are in good agreement with the data obtained for **3** in open cells. The efficiency of the cells sensitized with **1** was estimated to 7.4%.[27] Efficiencies of 4.7 and 2.9% were obtained for cells containing **3** plus additive and without additive, respectively. In the first twelve days after fabrication, the cell performances improved. The effect was much more pronounced for the cells containing the phenylcyanamide complex. The new efficiencies were estimated at 5.1 and 4.0%, respectively.

In the following, only the performance of cells containing **1** remained constant. For the cells sensitized with **3**, both current and voltage began to decrease, regardless of the presence of an additive. The degradation process was accompanied by dramatic losses in fill factor. For some of the cells, it was already at 0.4 mA cm^{-2} after 40 days of irradiation. After two months, the average photovoltage was at around 300 mV and currents were at 2 μA cm^{-2}. The standard deviation of these values was over 50%. It should be noted that the positive effect of the additive was no longer visible. Cells containing **3** without additive were superior in all parameters after two months of irradiation. In contrast, cells sensitized with **1** displayed an outstanding stability both in the current–voltage characteristics and the fill factor (see Fig. 7).

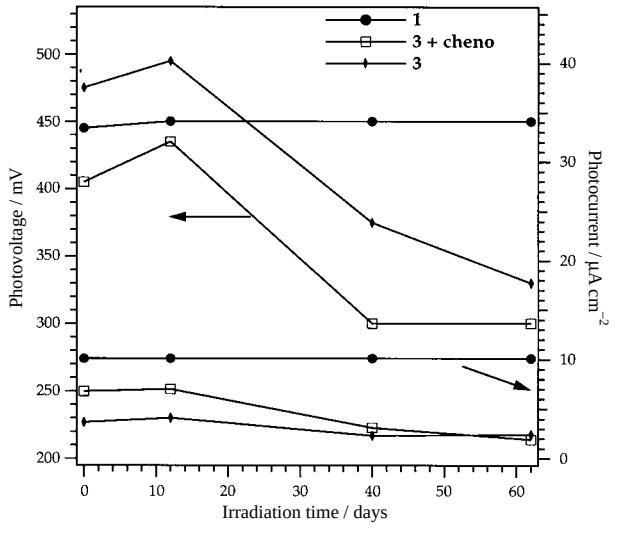

Fig. 7 Open-circuit voltage (upper curves) and short-circuit current (lower curves) monitored with time after exposure to 5000 lx at 50 °C and polycarbonate UV filter (average of five cells). Measurements were taken at 50 lx

Comparison of the dithiocyanate complex **1** and the diphenylcyanamide dye **3** in the same system reveals dramatic differences for the long term stability of the cells. With the results presented, a slow decomposition of **3** in the device appears likely. However, care must be taken with such an interpretation, as there are other possible explanations for the deteriorating performance. When a TiO_2 electrode is immersed in a solution of **3** without additive, surface aggregation takes place. This leads to the presence of small amounts of **3** not directly attached to the semiconductor, in the cell. As shown above, species in solution are not stable under irradiation. Their decomposition products might increase the dark current of the cell. The addition of cholanic acid efficiently controls the surface coverage with dye, but decomposition products of the additive might have the same detrimental effects on the dark current. The dark current influences the open-circuit voltage of the solar cell, and in more extreme cases, the fill factor of its maximum power point. Another source of instability might be the increased crystal water content of the phenylcyanamide dyes. In fact, the evolution of the short-circuit current of the cells containing **3** is very similar to that of cells of **1** containing some additional water.

With the experiments performed, it was not possible to determine the source of instability. Nevertheless, the system used was optimized in electrolyte and redox mediator concentration for an application of **1**, hence further efforts would have to be taken in order to optimize it for the diphenylcyanamide sensitizer. The existence of a stable system sensitized with **3** cannot yet be excluded.

Conclusions

The chemistry and photoelectrochemistry of ruthenium polypyridyl complexes containing two phenylcyanamide ligands was investigated. The compounds are structurally very similar to the most efficient known sensitizer, *cis*-$Ru(dcbpyH_2)_2(NCS)_2$, **1**. Due to the higher donor strength of the phenylcyanamide ligands, compared with thiocyanate, light absorption of the new complexes at longer wavelengths was improved. The use of two phenylcyanamide ligands caused a redshift of 14 to 30 nm of the ^{1}MLCT maximum.

In the preparation of some diphenylcyanamide complexes, linkage isomers occurred, containing one nitrile- and one amide-bound phenylcyanamide ligand. This was verified with ^{1}H and ^{13}C NMR spectroscopy.

Despite better light harvesting at lower energies, solar cell efficiencies of the new complexes were limited to values between 3 and 4%. This is due to reduced charge injection efficiencies at 540 nm (which are between 47 and 61%) and to relatively poor fill factors of the cells.

In the standard solar cell system, with a given semiconductor, electrolyte, and redox mediator, the diphenylcyanamide complexes appear not to be competitive with $Ru(dcbpyH_2)_2(NCS)_2$, although the positions of their ground and excited state energy levels should not prevent them from quantitative charge injection. Surface aggregation, which was not suppressed completely by additives, and reduced dye regeneration due to mass transport problems, might be responsible for the reduced IPCE values, compared with the dithiocyanate complex.

The stability of phenylcyanamide complexes under the influence of light was investigated. Irradiation of dye solutions in 0.25 M NaOH yielded an activation of the phenylcyanamide ligand and its fast replacement by hydroxide. The introduction of the strong electron donor hydroxide caused a strong red-shift of the MLCT bands in the UV/VIS spectra. In

methanol, the MLCT bands of the investigated complexes were blue-shifted under the influence of light. NMR spectra revealed phenylcyanamide complex decomposition, the formation of multiple new complexes, and the appearance of free cyanide.

Solar cell devices containing **3** degraded in long-term experiments. It appears likely that complex decomposition is responsible for the loss in performance, but an unambiguous conclusion is not possible, as there might be other reasons for cell degradation.

Acknowledgements

This research was financially supported by the Institut für Angewandte Photovoltaik, (INAP), Gelsenkirchen, Germany. Furthermore, it is a pleasure to acknowledge experimental help of Dr. Tobias Meyer (Solaronix SA), Dr. Marie Jirousek, and Stefanie Maier.

References

1 B. O'Regan and M. Grätzel, *Nature*, 1991, **353**, 737.
2 M. K. Nazeeruddin, A. Kay, I. Rodicio, R. Humphry-Baker, E. Müller, P. Liska, N. Vlachopoulos and M. Grätzel, *J. Am. Chem. Soc.*, 1993, **115**, 6382.
3 J. Desilvestro, M. Grätzel, L. Kavan, J. Moser and J. Augustynski, *J. Am. Chem. Soc.*, 1985, **107** 2988.
4 N. Vlachopoulos, P. Liska, J. Augustynski and M. Grätzel, *J. Am.Chem. Soc.*, 1988 **110**, 1216.
5 R. Amadelli, R. Argazzi, C. A. Bignozzi and F. Scandola, *J. Am. Chem. Soc.*, 1990, **112**, 7099.
6 R. Argazzi, C. A. Bignozzi, T. A. Heimer, F. N. Castellano and G. J. Meyer, *Inorg. Chem.*, 1994, **33**, 5741.
7 O. Kohle, S. Ruile and M. Grätzel, *Inorg. Chem.*, 1996, **35**, 4779.
8 S. Ruile, O. Kohle, P. Péchy and M. Grätzel, *Inorg. Chim. Acta*, 1997, in the press.
9 A. B. P. Lever, *Inorg. Chem.*, 1990, **29**, 1271.
10 P. A. Anderson, G. F. Strouse, J. A. Treadway, F. R. Keene and T. J. Meyer, *Inorg. Chem.*, 1994, **33**, 3863.
11 R. J. Crutchley, K. McCaw, F. L. Lee and E. J. Gabe, *Inorg. Chem.*, 1990, **29**, 2576.
12 N. Papageorgiou, Y. Athanassov, M. Armand, P. Bonhôte, H. Petterson, A. Azam and M. Grätzel, *J. Electrochem. Soc.*, 1996, **143**, 2999.
13 O. Kohle, M. Grätzel, T. Meyer and A. Meyer, *Adv. Mater.*, 1997, **9**, 904.
14 O. Kohle, PhD Thesis, No 1532, EPF Lausanne, 1996.
15 C. J. Barbé, F. Arendse, P. Compte, M. Jirousek, F. Lenzmann, V. Shklover and M. Grätzel, unpublished work.
16 P. Bonhôte, A. P. Dias, N. Papageorgiou, K. Kalyanasundaram and M. Grätzel, *Inorg. Chem.*, 1996, **35**, 1168.
17 R. J. Crutchley and M. L. Naklicki, *Inorg. Chem.*, 1989, **28**, 1955.
18 M. Grätzel and P. Liska, US Patent 5 084 365, 1992.
19 J. D. Birchall, J. R. Wood and T. D. Odonoghue, *Inorg. Chim. Acta*, 1979 **37**, L461.
20 A. R. Rezvani and R. J. Crutchley, *Inorg. Chem.*, 1994, **33**, 170.
21 M. L. Naklicki and R. J. Crutchley, *Inorg. Chem.*, 1989, **28**, 4226.
22 R. H. Herber, G. Nan, J. A. Potenza, H. J. Schugar and A Bino, *Inorg. Chem.*, 1989, **28**, 938.
23 S. Ruile, PhD Thesis No 1629, EPF Lausanne, 1997.
24 H. E. Toma and H. E. Malin, *Inorg. Chem.*, 1973, **12**, 1039.
25 A. A. Schilt, *J. Am. Chem. Soc.*, 1963, **85**, 904.
26 A. Kay and M. Grätzel, *J. Phys. Chem.*, 1993, **97**, 6272.
27 White light conversion efficiencies were estimated as follows: 120 000 lx $\approx$ 1000 W/m^2 $\Rightarrow$ 50 lx $\approx$ 0.42 W/m^2; $W_{in} \approx 0.42 \times 10^{-4}$ W/cm^2; $W_{out} \approx \mathrm{ff} \cdot U_{OC} \cdot I_{SC} = 0.70 \times 445 \times 10 \times 10^{-6}$ W/cm^2; $\eta = W_{out}/W_{in} \approx 7.4\%$.

Received 8*th April* 1997; *Paper* 7/06740B